Arch. Mech., 43, 5, pp. 565–575, Warszawa 1991

# Transitions to complex flows in thermal convection

F. H. BUSSE (BAYREUTH) and R. M. CLEVER (LOS ANGELES)

CONVECTION driven by thermal buoyancy in a layer heated from below represents the simplest kind of hydrodynamic instability. This simplicity manifests itself in the supercriticality of the onset of convection rolls and of all subsequent bifurcations that have been investigated so far. The transmitions to three-dimensional forms of convection are reviewed in this paper in dependence on the Prandtl number and their physical mechanisms are interpreted. Special attention is devoted to the cases of steady and oscillatory knot convection.

## 1. Introduction

THE COMPLEX dynamical processes involved in turbulent flows have challenged fluid dynamicists for over a century. Transitions to turbulence in particularly simple flow configuration such as plane Couette flow and pipe flow are difficult to investigate because bifurcations from the basic solutions have not been found. Even in the case of Poiseuille flow in a channel where the bifurcation in known (THOMAS, [14]; see also DRAZIN and REID, [12]) this knowledge is of limited use because the bifurcation is delayed owing to dynamical constraints and the experimental observations typically show a sudden onset of turbulence at much lower Reynolds numbers.

In terms of existing symmetries a fluid layer heated from below represents an even simpler configuration for the study of turbulence than those mentioned above. The energy source for the turbulent flow does not depend on the horizontal direction and the dependence on the vertical coordinate is the minimal dependence required for a turbulent state under steady conditions. Thermal convection in a layer of a Boussinesq fluid does indeed exhibit number features which reflect the simplicity of the energy source and the degree of symmetry of the geometrical configuration. The onset of convection and subsequent transitions to more complex forms of convection occur in the form of supercritical bifurcations such that the property of stability is usually taken over by the bifurcating solutions. This feature facilitates the numerical simulation of the evolution of convection flows with increasing Rayleigh number.

High degrees of symmetry of a problem are not only attractive because of the resulting simplifications of the mathematical analysis. They are often essential in the study of bifurcations because the latter are typically characterized by broken symmetries. In more general configurations without the respective symmetries, the bifurcations are replaced by imperfect bifurcations and transitions are no longer clearly identifiable because they occur gradually. We thus will focus in the analysis on the ways in which symmetries are broken as convection rolls become three-dimensional cellular motions or propagating waves and new degrees of motion are occupied in subsequent transitions.

There are two general conclusions that can be derived from a study of convection. The first statement concerns the mechanisms of the various instabilities of convection rolls which accomplish the transitions to three-dimensional flows. It is found that even when a three-dimensional flow has been introduced by one of these mechanisms, the other

mechanisms tend to reappear at higher transitions. The instabilities of rolls thus offer a typical picture of several of the mechanisms operating in turbulent convection. The second statement is that well defined structures and characteristic wavelengths are exhibited by turbulent convection even in the range of asymptotically high Rayleigh and Reynolds numbers. In this respect thermal convection defies the common notion that turbulence becomes a purely stochastic phenomenon in the limit of high Reynolds numbers. The best evidence in support of this statement comes from the observations of convection structures is strato-cumulus cloud layers, from mesoscale convection as visualized by satellite pictures (see Fig. 1, for example) or from the observation of the granulation and supergranulation at the surface of the sun. We shall return to the question of the coexistence of small scale chaotic media with large steady structures in the concluding remarks.

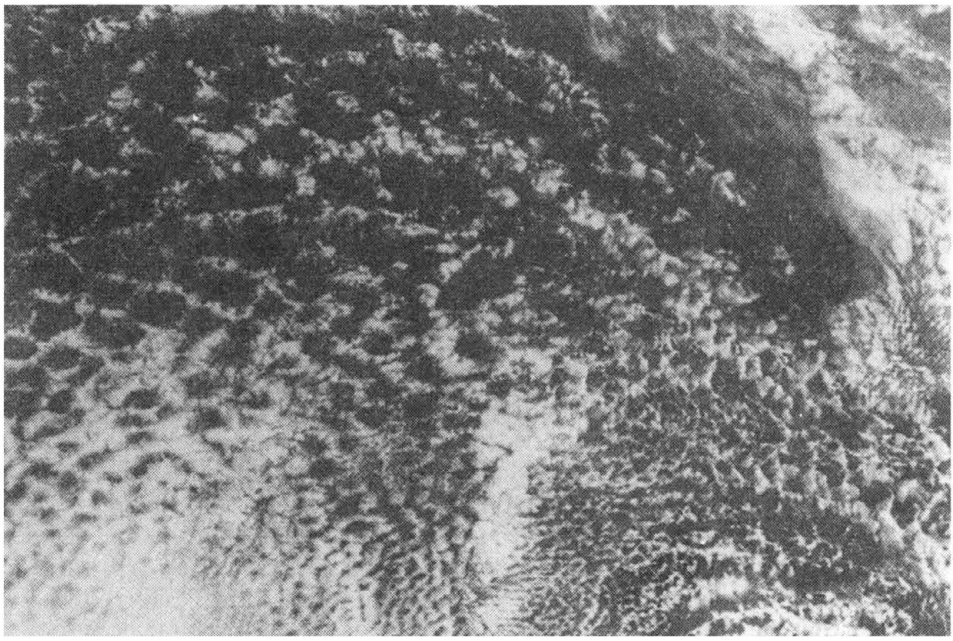

FIG. 1. Mesoscale convection over the South Atlantic (from BRIMACOMBE [6]).

## 2. Steady convection rolls

We consider a horizontal fluid layer of height $d$ with no-slip boundaries on which the temperatures $T_1$ and $T_2$ are prescribed with the higher value $T_2$ on the bottom boundary. A sketch of the geometrical configuration is shown in Fig. 2. Using $d$ as length scale, $d^2/\kappa$ as time scale, where $\kappa$ is the thermal diffusivity and $T_2 - T_1$ as scale of the temperature, the equation of motion for the velocity vector $\mathbf{u}$ and the heat equation for the deviation $\theta$ from the static solution of pure conduction can be written in the form

$$\nabla^2\mathbf{u} + R\theta\mathbf{k} - \nabla\pi = \left(\mathbf{u}\cdot\nabla\mathbf{u} + \frac{\partial}{\partial t}\mathbf{u}\right)P^{-1},$$

$$\nabla\mathbf{u} = 0, \tag{2.1}$$

(2.1) [cont.)
$$\nabla^2\theta + \mathbf{k}\cdot\mathbf{u} = \mathbf{u}\cdot\nabla\theta + \frac{\partial}{\partial t}\theta,$$

where **k** is unit vector in the vertical direction, and the Rayleigh number $R$ and the Prandtl number $P$ are defined by

$$R = \frac{\gamma g(T_2 - T_1)d^3}{\kappa\nu}, \qquad P = \frac{\nu}{\kappa}.$$

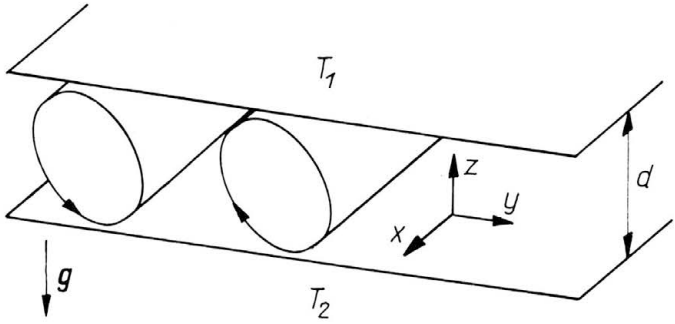


FIG. 2. Geometrical configuration of the convection layer.

Here we have denoted the thermal expansivity by $\gamma$, the acceleration of gravity by $g$ and the kinematic viscosity by $\nu$. The boundary conditions of the problem we are considering are given by

(2.2)
$$\mathbf{u} = \theta = 0, \quad \text{at} \quad z = \pm\frac{1}{2}.$$

We use a Cartesian system of coordinates with $z$-coordinate in the vertical direction and consider two-dimensional solutions since those are the only ones which are stable at Rayleigh numbers close to the critical value for onset of convection (SCHLÜTER *et al.*, 1965).

The deviation $\theta$ of the temperature from the distribution in the state of pure conduction will be used in the following as the representative dependent variable of the convection flow. Using the $x$-coordinate in the direction of the axis of the rolls we can write the solution for $\theta$ in the form

(2.3)
$$\theta = \sum_{m,n} b_{mn} \cos m\alpha y \sin n\pi\left(z + \frac{1}{2}\right).$$

Anticipating that the solutions of interest possess a vertical plane of symmetry, we have located the origin on the intersection between such a plane and the median plane of the layer. Since we have assumed a Boussinesq fluid and symmetric boundary conditions we find that the convection rolls bifurcating from the static solution of the problem at the critical Rayleigh number $R_c$ satisfy the additional symmetry property

(2.4)
$$\theta(y, z) = -\theta\left(\frac{\pi}{\alpha} - y, -z\right).$$

According to this property all coefficients $b_{mn}$ with odd $m+n$ vanish in the representation (2.3). Solutions of the form (2.3) can be obtained for a wide range of the $R - \alpha - P$ parameter space, $R$ is the Rayleigh number and $P$ is the Prandtl number. We refer to

BUSSE [2], CLEVER and BUSSE [7, 8], BUSSE and CLEVER [4] and BOLTON, BUSSE and CLEVER [1].

An important consideration in the numerical computations of solutions of the form (2.3) is the truncation of the infinite sums. We have generally used the truncation condition, that all coefficients and corresponding equations with

$$n + m > N_T \tag{2.5}$$

are neglected. In the computations of the three-dimensional solutions discussed in Sects. 4 and 5 the left-hand side must be replaced by $n + m + l$. By changing $N_T$ in steps of two, quality of the numerical approximations can be compared. $N_T$ is regarded as sufficiently large when no significant changes in sensitive physical properties such as the convective heat transport are noticed after a replacement of $N_T$ by $N_T + 2$.

## 3. Instabilities of convection rolls

General three-dimensional infinitesimal disturbances of the steady solution given by Eqs. (2.1) can be written in the form

$$\theta = \sum_{m,n} b_{mn} \exp\{im\alpha y + idy + ibx + \sigma t\} \sin n\pi \left(z + \frac{1}{2}\right), \tag{3.1}$$

where Floquet's theorem has been used. Because of property (2.4) the general disturbances of the form (3.1) separate into two classes. Those of class $E$ have vanishing coefficients $b_{mn}$ for odd $n + m$, while the coefficients of class 0 vanish for even $n + m$. It turns out that the real part of the growth-rate $\sigma$ often reaches a maximum for $d = 0$ in which case an additional symmetry appears. The disturbances can be separated in this case into those that are symmetric in $y$ and those that are antisymmetric. We shall denote the former subclass by $C$ (for cosine) and the latter subclass by $S$ (for sine). All types of disturbances that have been determined as instabilities of the steady roll solution (2.3) are listed in Table 1. As is evident from this table, most of the instabilities of convection rolls can be distinguished by their symmetry property if the symmetry in time is also included. But the knot- and the crossroll-instabilities have the same symmetry properties and can be distinguished as two separate maxima of the growth-rate $\sigma$ as a function of $b$ when instabilities listed in Table 1 are shown in Fig. 3. For details of the analysis we refer to

**Table 1. Properties of instabilities of convection rolls in a layer with rigid boundaries. The quantity $2\pi/\Omega$ is a measure of the circulation time in rolls.**

| Instability | Symmetry class | $b$ | $d$ | $\sigma_i$ | Symbol |
|---|---|---|---|---|---|
| cross-roll | $OC$ | $> \alpha_c$ | 0 | 0 | CR |
| knot | $OC$ | $< \alpha_c$ | 0 | 0 | KN |
| dual-blob | $OC$ | $< \alpha_c$ | 0 | $-2\Omega$ | DB |
| zig-zag | $ES$ | $< \alpha_c$ | 0 | 0 | ZZ |
| oscillatory | $ES$ | $< \alpha_c$ | 0 | $-\Omega$ | OS |
| single-blob | $EC$ | $> \alpha_c$ | 0 | $-\Omega$ | SB |
| skewed-varicose | $E$ | $\ll \alpha_c$ | $\ll \alpha_c$ | 0 | SV |
| Eckhaus | $E$ | 0 | $\ll \alpha_c$ | 0 | EC |

the above-mentioned papers in which the stability diagrams have been obtained for special values of the Prandtl number. Using those results and a few diagrams of stability boundaries for fixed values of $\alpha$ and $R$ surfaces drawn in Fig. 3 have been obtained by interpolation.

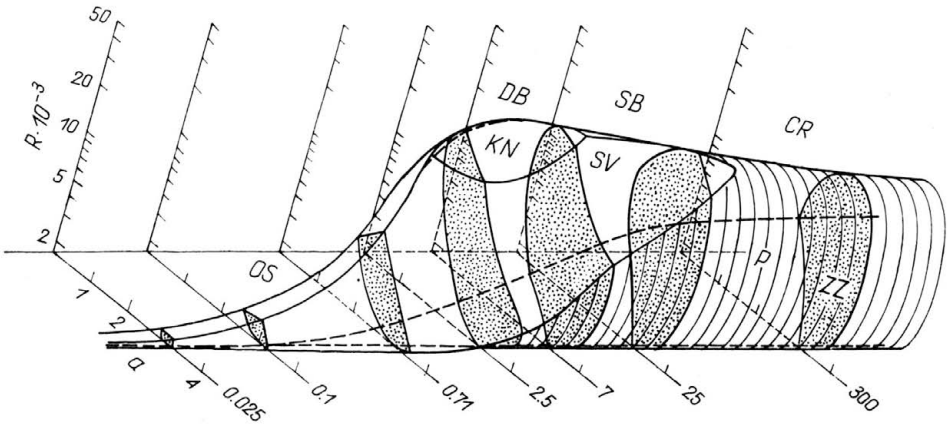


FIG. 3. Region of stable roll solution in the $R - \alpha - P$–parameter space.
The stability region is bounded by several surfaces corresponding to the instabilities listed in Table 1.

## 4. Three-dimensional solutions in the form of knot convection

Except for the Eckhaus instability all instabilities of Table 1 lead to three-dimensional forms of convection. In all cases with $d = 0$ the resulting convection flow assumes a regular pattern at least in the ideal case of uniformly excited disturbances. In the case of the skewed varicose instability it is not clear whether it can lead to a spatially periodic pattern of convection. If such a pattern exist it is likely to be unstable.

The simplest form of three-dimensional convection bifurcating from two-dimensional rolls is bimodal convection. This form of convection predominates in high Prandtl number fluids at Rayleigh numbers above $2 \cdot 10^4$. For experimental and theoretical studies of this form of convection we refer to BUSSE and WHITEHEAD [5], WHITEHEAD and CHEN [15] and FRICK *et al* [13]. In terms of symmetry properties the transition to steady knot convection induced by the knot instability is analogous to the transition to bimodal convection; the actual appearance of the two types of three-dimensional convection is quite different, however. In Fig. 4 a typical example of knot convection is shown. The concentration of the rising and falling fluid into thin plumes is a characteristic feature of knot convection and is responsible for its name since the plumes become visible as "knots" is the shadow-graph observations (BUSSE and CLEVER [4]). The collection of fluid from the hot and cold thermal boundary layer into up- and down-drafts tends to improve the heat transport. Because of the high momentum with which those plumes impinge on the opposite boundary, steep temperature gradients are created which result in an effective heat transport. At higher Rayleigh number spoke-like structures corresponding to fluid

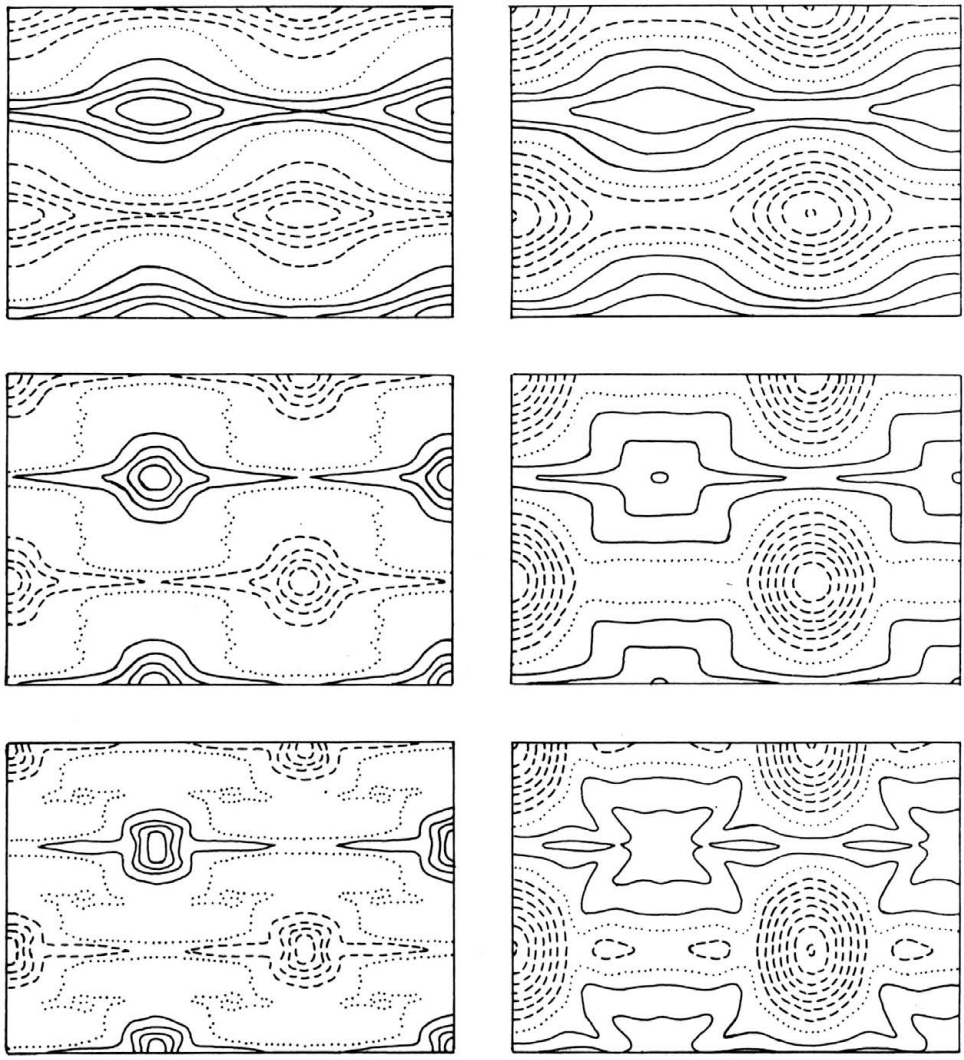

FIG. 4. Steady knot convection with $\alpha_x = 1.7$, $\alpha_y = 2.5$ for $P = 2.5$ and different values of $R$, $1.5 \cdot 10^4$ (middle row) and $10^5$ (lower row).The isotherms in the plane $z = 0$ are shown on the left side and $\partial(\theta - \overline{\theta}/\partial z$ at $z = -0.5$ is shown on the right hand side, where $\overline{\theta}$ is the horizontally averaged component of $\theta$.

breaking away from the thermal boundary layers become noticeable around the stems of the plumes. These spokes indicate that knot-convection is a representative example of spoke pattern convection which is the ubiquitous form of convection observed in experiments with fluids of moderate Prandtl numbers for Rayleigh numbers from a few times $10^4$ up to $10^7$.

In the experimentally realized spoke pattern convection the spokes are strongly time-dependent and the origin of this time-dependence can be traced to hot or cold blobs of fluids circulating around with the convection velocity. This kind of time dependence originates from the blob instabilities listed in Table 1. Since they occur in the same general

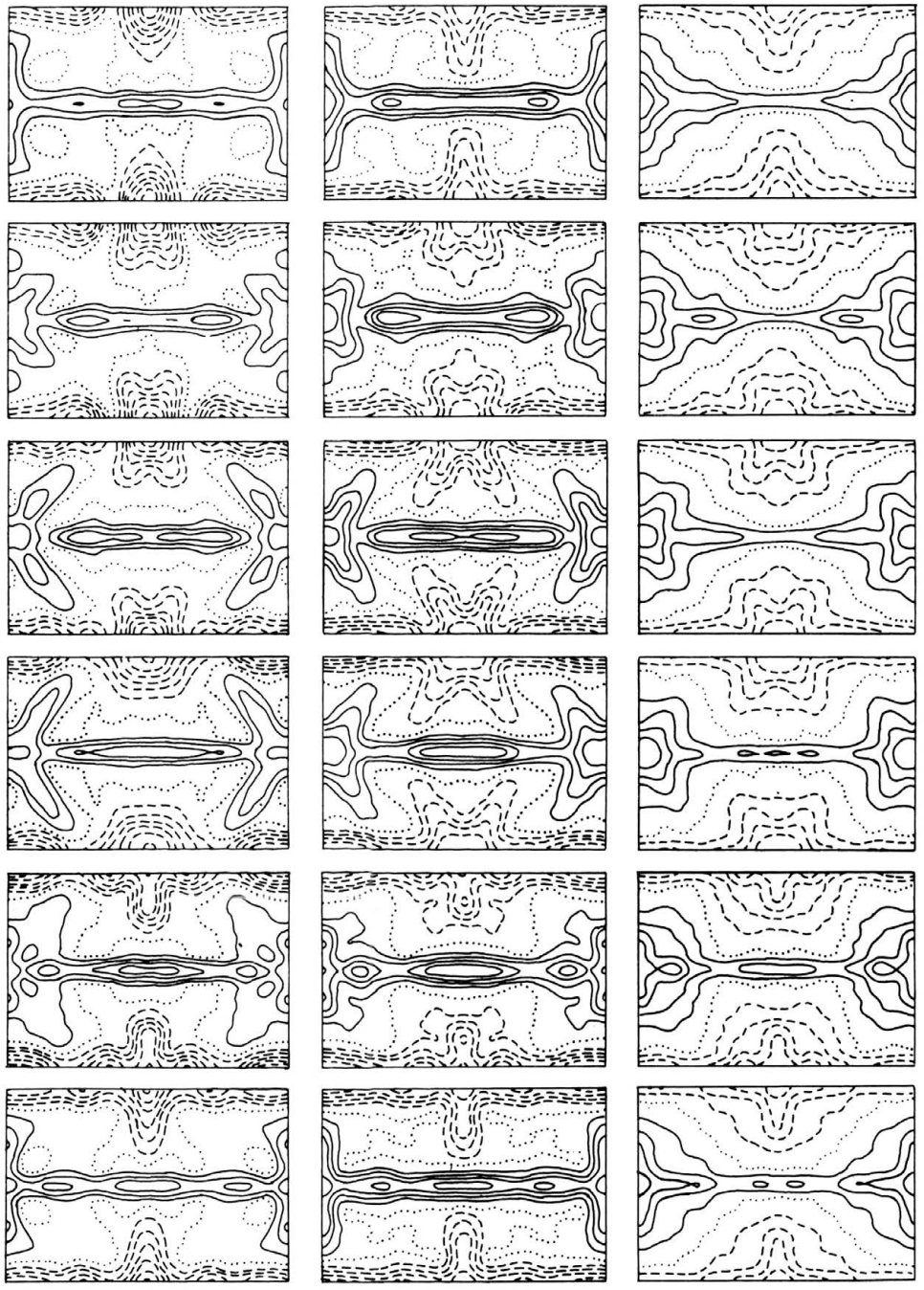

FIG. 5. Oscillatory knot convection at $R = 4 \cdot 10^4$, $P = 2.5$ with $\alpha_y = 2.0$, $\alpha_x = 1.4$. The upper and middle rows show values of constant $u_z$ in the planes $z = -0.3$ and $z = 0$, respectively. The lower row shows the vertical average of the temperature $\int_{-1/2}^{1/2} \theta dz$. In each row pictures are separated by $\Delta t = 0.05$ in time. The total time span covers nearly one period, $T = 0.085$. The instability of the steady knot solution which has given rise to the oscillatory knot convection shown in this figure is of the $ECS$-type.

parameter regime as the knot instability, it is not surprising that they reappear as instabilities of steady knot convection once the latter form of convection has been established. Conversely, the characteristic features of knot convection will appear when the transition from rolls to standing blob oscillations has occurred first. But this latter case can not be investigated as easily since the blob instabilities break two symmetries at once, namely the invariances with respect to translation along the axis of the rolls and with respect to translation in time.

Since steady knot convection can be described by an expression for $\theta$ of the form

$$\theta = \sum_{l,m,n} b_{lmn} \cos l\alpha_x x \cos m\alpha_y y \sin n\pi \left(z + \frac{1}{2}\right), \tag{4.1}$$

where non-vanishing coefficients $b_{lmn}$ are obtained only for even $l + m + n$, the general disturbances of the form

$$\theta = \sum_{l,m,n} b_{lmn} \exp\{il\alpha_x x + idx + im\alpha_y y + iby + \sigma t\} \sin n\pi \left(z + \frac{1}{2}\right) \tag{4.2}$$

separate in two classes, those with non-vanishing coefficients $b_{lmn}$ for even $l + m + n$ and those with odd $l + m + n$. In the special case $b = d = 0$ additional symmetries with respect to the $x$- and $y$-dependences of the disturbances are realized and eight different types of instabilities can be distinguished,

$$ECC,\ ESC,\ ECS,\ ESS,\ OCC,\ OSC,\ OCS,\ OSS. \tag{4.3}$$

The notation used is analogous to that introduced in Table 1 in that the first $C$ or $S$ denotes symmetry or antisymmetry in $x$ while the last letter does the same with respect to the $y$-dependence. According to experimental observations the most important instabilities do indeed correspond to case $b = d = 0$ and the computations of CLEVER and BUSSE [10] have thus been restricted to this case. A special property of the istabilities with $CS$ or $SC$ in Eq. (3.3) is that they include a mean flow component which is symmetric with respect to the median plane $z = 0$ in the case of the class $E$ and antisymmetric in the case of class 0. Such the property is not realized for the istabilities of Table 1 since those occur all for finite values $b$ or $d$. Instabilities corresponding to every subset listed in Eq. (3.3) seem to occur in the case of knot convection depending on the parameters $\alpha_x$, $\alpha_y$, and $P$. The mechanism of instability is similar to the dual blob instability of Table 1 in all cases and only phase relationships differ somewhat for the different cases (3.3). An example of oscillatory knot convection induced by the $ECS$ instability is shown in Fig. 5.

## 5. Travelling wave convection

Symmetric traveling wave convection is realized through the Hopf bifurcation from steady rolls in form of the oscillatory instability. In the frame of reference moving with wavespeed $c$ the solution describing travelling wave convection becomes steady,

$$\theta = \sum_{lmn} \{b_{lmn} \cos l\alpha_x(x - ct) + \hat{b}_{lmn} \sin l\alpha_x(x - ct)\} \begin{Bmatrix} \cos m\alpha_y y \\ \sin m\alpha_y y \end{Bmatrix} \sin n\pi \left(z + \frac{1}{2}\right), \tag{5.1}$$

where the upper function in the wavy bracket applies for even $l$ and the lower function corresponds to odd $l$. As in the case of rolls the coefficients $b_{lmn}$ and $\hat{b}_{lmn}$ are non-vanishing only for even $m + n$. A typical example of finite amplitude travelling wave

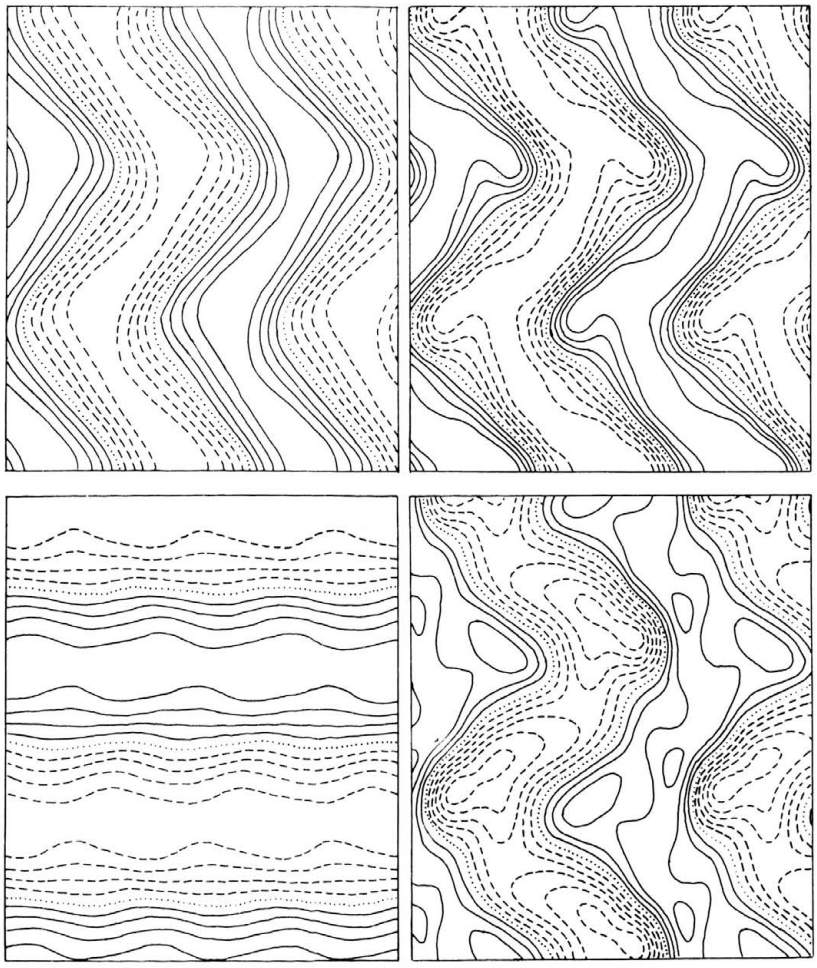

FIG. 6. Travelling wave convection with $\alpha_x = 2.2$, $\alpha_y = 2.6$ for $P = 0.1$, $R = 3500$. Lines of constant vertical velocity in the planes $z = 0$ (upper left) and $z = 0.3$ (upper right) and lines of constant $\int_{-1/2}^{1/2} \theta dz$ (lower left) and of constant $\psi$ at $z = 0$ (lower right) are shown. The waves travel towards the right.

convection is shown in Fig. 6. It is worth noting that a symmetric mean flow along the $x$-direction is associated with the travelling wave and that it is proportional to the square of the wave amplitude as long as the latter is sufficiently small. While the mean flow is almost negligible at the Prandtl number of air, it can become quite important in low Prandtl number convection (CLEVER and BUSSE [10]). In the analysis of the stability of symmetric travelling wave convection, symmetry properties can be used again if the analysis is restricted to disturbances fitting the same horizontal periodicity interval as the travelling wave solution. Four classes of disturbances can be distinguished when the representation

$$\theta = \sum_{l,m,n} [(b_{lmn} \cos l\alpha_x(x - ct) + b_{lmn} \sin l\alpha_x(x - ct)] \begin{Bmatrix} \sin m\alpha_y y \\ \cos m\alpha_y y \end{Bmatrix} \sin n\pi \left(z + \frac{1}{2}\right) e^{\sigma t} \tag{5.2}$$

for the disturbance temperature field is assumed. The summation over $m$, $n$ can be extended over either non-negative integers with even $m + n$ or those with odd $m + n$, and the upper function in the wavy bracket can be chosen for odd $l$ and the lower function for even $l$ as in the case of the symmetric travelling wave solution, or the choice can be made the other way around. In the analysis of CLEVER and BUSSE [9, 11] it is found that only disturbances exhibiting the symmetry opposite to that of symmetric traveling wave convection in both respects give rise to grow-rates $\sigma$ with positive real parts in the parameter regime that has been investigated. For Prandtl numbers of the order unity these disturbances lead to asymmetric travelling wave convection while for small Prandtl numbers of the order 0.1 or smaller a transition to standing oscillations takes place. Experimental observations for the latter phenomenon do not seem to be available yet, however.

## 6. Concluding remarks

As thermal convection evolves from simple rolls towards more complex patterns, various degrees of freedom of motion become occupied such as vertical vorticity, time dependence and mean flow components of motion all of which vanish for rolls. The new degrees of freedom are introduced by a variety of instabilities which break one or more of the remaining symmetries of the convection flow. At moderate and high Prandtl numbers the thermal boundary layers play a crucial role in the mechanisms of instability while for low Prandtl number fluids the momentum advection terms exert a dominant influence. The horizontally periodic convection flows reviewed in this paper represent idealized solutions that can be realized in laboratory experiments with controlled initial conditions. These solutions retain a maximum of symmetries at each step of the evolution of nonlinear convection and thereby they permit a separation of different mechanisms of instability. In experimental situations where initial conditions are not prepared appropriately, symmetries are realized only approximately and thus most of the transitions correspond to imperfect bifurcations. In some instances small asymmetries can play an important role in triggering transitions. The transition to time-dependent convection in high Prandtl number fluids is an example for this effect as is discussed in BUSSE [3]. Nevertheless, the analysis of strictly periodic patterns must precede systematic attempts to understand transitions in more general patterns.

The coexistence of the small scale oscillatory motion and the large scale stationary convection pattern seen in the Fig. 5 for oscillatory knot convection is also typical for experimental observations of spoke pattern convection (BUSSE [3]). In movies that have been made by the first author a stationary network of large scale square cells (with sides of approximately 10 $d$) remains visible up to Rayleigh numbers of several millions. The corners of these cells represent the plumes towards which the thermals erupting from the thermal boundary layers are collected and by which they are carried to the opposite boundary. To some extent the sides of the square cell participate in this process in that they represent sheets of rising and falling fluid in competition with the much stronger plumes at the corners. Descending and rising large scale motions are 90° out of phase

such that the cold plumes are located at the center between four hot plumes. In all qualitative aspects spoke pattern thus resembles the oscillatory knot convection as shown in Fig 5 except that through the difference in the $x$- and $y$-dependence the origin from the convection rolls is still visible in those pictures.

The most impressive aspect of turbulent spoke pattern convection is the way in which the steady large scale cellular network organizes the small scale chaotic motions emerging from the unstable thermal boundaries. In this respect the laboratory experiment resembles the large scale convection cells in planetary and stellar convection zones with their often well defined wavelength. The processes that determine these wavelength are not known and represent a fascinating topic of research.

The research reported in this paper has been supported by the Atmospheric Sciences Section of the U.S. National Science Foundation.

## References

1. E. W. BOLTON, F. H. BUSSE and R. M. CLEVER, *Oscillatory instabilities of convection rolls at intermediate Prandtl numbers*, J. Fluid Mech., **164**, 469–485, 1986.
2. F. H. BUSSE, *On the stability of two-dimensional convection in a layer heated from below*, J. Math. Phys., **46**, 140–150, 1967.
3. F. H. BUSSE, *Nonlinear properties of convection*, Rep. Progress Phys., **41**, 1929–1967, 1978.
4. F. H. BUSSE and R. M. CLEVER, *Instabilities of convection rolls in a fluid of moderate Prandtl number*, J. Fluid Mech., **91**, 319–335, 1979.
5. F. H. BUSSE and J. A. WHITEHEAD, *Instabilities of convection rolls in a high Prandtl number fluid*, J. Fluid Mech., **47**, 305–320, 1971.
6. L. A. BRIMACOMBE, *Atlas of meteosat imagery*, European Space Agency, 1981.
7. R. M. CLEVER and F. H. BUSSE, *Transition to time-dependent convection*, J. Fluid Mech., **65**, 625–645, 1974.
8. R. M. CLEVER and F. H. BUSSE, *Large wavelength convection rolls in low Prandtl number fluids*, J. Appl. Math. Phys., ZAMP, **29**, 711–714, 1978.
9. R. M. CLEVER and F. H. BUSSE, *Nonlinear oscillatory convection*, J. Fluid Mech., **176**, 403–417, 1987.
10. R. M. CLEVER and F. H. BUSSE, *Three-dimensional knot convection in a layer heated from below*, J. Fluid Mech., **198**, 345–363, 1989.
11. R. M. CLEVER and F. H. BUSSE, *Nonlinear oscillatory convection in the presence of a vertical magnetic field*, J. Fluid Mech., **201**, 507–523, 1989.
12. P. DRAZIN and W. REID, *Hydrodynamic stability*, Cambridge University Press, 1981.
13. H. FRICK, F. H. BUSSE and R. M. CLEVER, *Steady three-dimensional convection at high Prandtl number*, J. Fluid Mech., **127**, 141–153, 1983.
14. L. H. THOMAS, *The stability of plane Poiseuille flow*, Phys. Rev., **91**, 780–783, 1953.
15. J. A. WHITEHEAD and G. L. CHAN, *Stability of Rayleigh-Bénard convection rolls and bimodal flow at moderate Prandtl number*, Dyn. Atmosph. Oceans., **1**, 33–49, 1976.

**INSTITUTE OF PHYSICS**
**UNIVERSITY OF BAYREUTH, GERMANY**
**and**
**INSTITUTE OF GEOPHYSICS AND PLANETARY PHYSICS**
**UCLA, LOS ANGELES, USA.**

*Received August* 26, 1991.